Efficient Simulation of Cascading Outages Using an Energy Function-Embedded Quasi-Steady-State Model

Zhenping Guo, *Student Member*, *IEEE*, Xiaowen Su, Kaiyang Huang, *Student Member*, *IEEE*, Kai Sun, *Fellow*, *IEEE*, Srdjan Simunovic, Hsiao-Dong Chiang, *Life Fellow*, *IEEE*

***Abstract*—This paper proposed an energy function-embedded quasi-steady-state model for efficient simulation of cascading outages on a power grid while addressing transient stability concerns. Compared to quasi-steady-state models, the proposed model incorporates short-term dynamic simulation and an energy function method to efficiently evaluate the transient stability of a power grid together with outage propagation without transient stability simulation. Cascading outage simulation using the proposed model conducts three steps for each disturbance such as a line outage. First, it performs time-domain simulation for a short term to obtain a post-disturbance trajectory. Second, along the trajectory, the system state with the local maximum potential energy is found and used as the initial point to search for a relevant unstable equilibrium by Newton's method. Third, the transient energy margin is estimated based on this unstable equilibrium to predict an out-of-step condition with generators. The proposed energy function-embedded quasi-steady-state model is tested in terms of its accuracy and time performance on an NPCC 140-bus power system and compared to a quasi-steady-state model embedding transient stability simulation.**

***Index Terms*—Cascading outages, quasi-steady-state model, transient stability, energy function, transient energy margin.**

NOMENCLATURE

$n_{\max}$	Number of cascades
ω_s	Synchronous speed of the system
δ_i, ω_i	Rotor angle and speed of generator i
e'_{di}, e'_{qi}	d- and q-axis transient voltages
E_{fdi}	Field voltage
P_{mi}, P_{ei}	Mechanical and electrical powers
D_i, H_i	Damping coefficient and inertia
i_{di}, i_{qi}	d- and q-axis stator currents
X_{di}, X_{qi}	d- and q-axis synchronous reactances
X'_{di}, X'_{qi}	d- and q-axis transient reactances
T'_{d0i}, T'_{q0i}	d- and q-axis open-circuit time constants
T_{Ei}, T_{Gi}	Exciter and governor time constants
P_{refi}, R_i	Reference power and speed regulation of the governor
V_{refi}, E_{ti}, K_{Ai}	Reference voltage, terminal voltage, and the control gain of the exciter
D_{ei}	Equivalent damping coefficient modeling all frequency-dependent power changes including governor influence
E_i	Electromotive force behind X_{di}
R_{ai}	Stator resistance of generator i
$\tilde{E}_{ti0}$, $\tilde{I}_{ti0}$	Initial terminal voltage and current at generator bus i
λ	Uniform damping for all generators
G_{ij}, B_{ij}	Transfer conductance and susceptance between buses i and j in the Kron-reduced network
V_{KE}, V_{PE}, V_{cr}	Kinetic energy, potential energy, and critical energy
ΔV	Energy margin
$k_{\max}$	Maximum allowable number of searches
$\mathbf{x}_s$	Post-disturbance stable equilibrium
$\mathbf{x}_k^*$	k^{th} local maximum point of the potential energy on the short-term post-disturbance trajectory
$\mathbf{x}_{cr}$	Relevant unstable equilibrium
$\vec{\mathbf{e}}_k$, h	Search direction and step size
$\mathbf{p}_M$	M^{th} search point
$\mathbf{x}_{crk}$	First local maximum point of the potential energy along the search path $\vec{\mathbf{e}}_k$
$\Delta\delta_{\max}$	Maximum angle separation between any two generators
δ_u	Predefined threshold of angle separation for an unstable system
$\dot{x}$	Vector of derivatives of all state variables
$T_{\max}$	Transient stability simulation period

This work was supported in part by NSF grant ECCS-2329924, in part by the ISSE seed grant of the University of Tennessee, and in part by UT-Battelle, LLC, under Contract No. DE-AC05-00OR22725 with the U.S. Department of Energy.

Z. Guo, K. Huang and K. Sun are with the Department of EECS, University of Tennessee, Knoxville, TN, 37996, USA (e-mail: zguo19@vols.utk.edu, khuang12@vols.utk.edu, kaisun@utk.edu).

X. Su is with ISO New England, 55 Helmsford Way, Windsor, CT, 06095, USA (e-mail: xsu@iso-ne.com).

S. Simunovic is with the Computational Sciences and Engineering Division, Oak Ridge National Laboratory, Oak Ridge, TN, 37830, USA (e-mail: simunovics@ornl.gov).

H. D. Chiang is with the School of ECE, Cornel University, Ithaca, NY, 14853, USA (e-mail: hc63@cornell.edu).

I. INTRODUCTION

POWER grids are among the most complex interconnected engineering systems. Due to vast interconnections of power systems, even a small failure in power grids may propagate far away and lead to cascading outages. Cascading outages in power grids pose great threats to system security and reliability. Serious cascading outages could lead to widespread, severe

impacts both economically and socially. Therefore, modeling cascading outages is of great interest in uncovering their evolutionary patterns and further identifying effective mitigation strategies.

Modeling cascading outages is quite a challenging task because the pattern in which cascading outages propagate is often uncertain, involves lots of components and manifests multi-timescale dynamics. Generally speaking, there are two types of models on the cascading process: stochastic models and physical models. The main difference between these two is that the stochastic models do not model any power grid details including topological information, whereas the physical models require the modeling of the power grid topology and physical constraints, such as power flow equations. The stochastic models focus on key patterns in outage propagation, established offline based on large amounts of historical or simulated outage data without requiring detailed physical information of power systems. The models of this type are such as the CASCADE model [1], branching process model [2]-[3], interaction models [4]-[6] and influence graph models [7]-[8]. The physical models are required when detailed mechanisms or grid behaviors in the cascading process need to be simulated, and hence such models are established based on power system models. Existing physical models are such as the OPA (ORNL-PSerc-Alaska) model [9]-[13], the Manchester model [14], the hidden failure model [15], the COSMIC model [16], the Dynamic PRA model [17]-[18], and the multi-timescale model [19]. Most physical models on cascading processes adopt steady-state or quasi-steady-state power flow models for efficient simulations, ignoring transient dynamics of generators and other dynamic devices and the transitioning of the system from one steady-state condition to another after each failure or switch.

When the transient stability and detailed dynamics of a power grid under cascading outages are also of interests, some steady-state physical models can interface with dynamic simulations. For example, the enhanced OPA model discussed in [13] interfaces the steady-state power flow model of the grid with a transient stability simulator running on a detailed dynamic grid model, which enables assessing the system's transient stability and dynamic security following each component failure during the cascading process. However, the resulting cascading outage simulation that incorporates detailed dynamic simulations is computationally expensive and inefficient, particularly for large-scale power grids.

For efficient transient stability assessment (TSA) of a power system subjected to disturbances, the direct methods [20]-[30] based on the Lyapunov stability criterion are preferable alternatives to transient stability simulations. The direct methods find a Lyapunov function to determine the domain of attraction (DOA) about the stable equilibrium point (SEP) of the post-disturbance system, by which transient stability can be directly assessed without solving the system's detailed trajectory. However, finding a rigorous Lyapunov function for realistic power grid models is quite challenging if not impossible. Some direct methods construct local Lyapunov functions only for a small neighborhood of the SEP by convex programming [23]-[26]. Thus, a stability region can be approximately determined but is typically much smaller than the actual DOA and can result in conservative stability assessment. Instead, other direct methods adopt an energy function, which is an approximate Lyapunov function, by which the critical energy of the system without loss of transient stability may take the energy function's value at an unstable equilibrium point (UEP) such as the closest UEP from the SEP or a controlling UEP (CUEP) [27]-[28]. A widely known direct method is the BCU (boundary of stability region-based CUEP) method [21], which utilizes the computed fault-on trajectory to find the CUEP of an artificial reduced-dimension system model whose stability region is highly related to that of the original system, thereby simplifying the computation. Although the closest UEP can also be computed via the reduced system, the result tends to be more conservative than that of the BCU method. Compared to simulation-based TSA methods [31]-[32], direct methods are highly efficient because they do not require explicitly solving the dynamic trajectories of the system if an appropriate energy function is defined for acceptable accuracy of TSA [20]-[21].

For accurate and efficient cascading outage simulations addressing transient stability criteria, this paper proposes an energy function-embedded quasi-steady-state model (for short, an EF-QSS model). Specifically, an energy function method is integrated into the framework of the quasi-steady-state cascading model to determine whether the system may securely transition to a new SEP without encountering transient instability after each outage. In fact, the proposed energy function-embedded method can be implemented on any quasi-steady-state model for cascading outage simulations. The OPA model and its variants have been widely used to generate cascading outage data, understand the propagation mechanisms of cascading outages, and validate mitigation strategies [4], [6], [9], [10]. Without loss of generality, the OPA model [10] is employed in this paper to show how to implement the energy function-embedded method on a quasi-steady-state model and verify the effectiveness of the proposed EF-QSS model. The OPA model considers quasi-steady-state behaviors of a power grid in two timescales: the "slow dynamics" module simulates long-term grid upgrades with load growth, and the "fast dynamics" module simulates cascading outages and remedial control based on an optimal power flow (OPF) model ignoring transient dynamics. The proposed EF-QSS model interfaces the "fast dynamics" module with an energy function method that finds a relevant UEP to assess transient stability. It inherits the high efficiency of the OPA model for simulating the cascading process while addressing transient stability criteria with each failure or switch. The main contribution of this paper is that it develops an EF-QSS model, which integrates an energy function method into a quasi-steady-state power system model of the simulation of cascading outages. This integration can be implemented on any quasi-steady-state model, enabling accurate and efficient simulations of cascading outages that address transient stability criteria. In a quasi-steady-state model simulating cascading outages, each line outage is caused by an overload rather than a short-circuit fault. Consequently, there is no fault-on trajectory as required by the BCU method for TSA,

making it difficult to apply the BCU method directly in cascading outage simulations. To address this, the paper proposes obtaining a post-disturbance trajectory, instead, by conducting a short-term time-domain simulation to find a relevant UEP for the line outage. Existing physical simulation models of cascading outages either use steady-state or quasi-steady-state power flow models, ignoring the fast transient dynamics, or rely on computationally expensive time-domain simulations. As a result, there is a gap in the availability of a model that can simultaneously achieve both accuracy and computational efficiency in simulating cascading outages. The proposed EF-QSS model bridges this gap by offering a balanced solution that accounts for transient stability while maintaining accuracy and efficiency.

In the rest of the paper, section II presents the flowchart of the proposed EF-QSS model and introduces the power system model and the energy function method employed. Then, section III provides comprehensive case studies on a Northeast Power Coordinating Council (NPCC) 140-bus system to evaluate the accuracy and time performance of the EF-QSS model and compares it with the original OPA model and the enhanced OPA model that incorporates transient stability simulations. Finally, section IV draws conclusions of the paper.

II. Proposed EF-QSS Model

A. Flowchart of the EF-QSS Model

The flowchart of the EF-QSS model is shown in Fig. 1, which integrates the "fast dynamics" module of the OPA model in the blue box on the right-hand side and the energy function module in the green box on the left-hand side. Following each line outage, the OPA model calculates power flows to check line overloading and conducts line protection or mitigation control such as generation redispatch and load shedding based on a DC OPF model. The energy function module checks the stability of the system following each line outage and takes remedial control to trip unstable generators.

In the existing framework of the OPA model considering the fast dynamics shown in the box on the right-hand side of Fig. 1, a cascade event is triggered by an initial outage, such as random line outages, and the DC power flow of the post-disturbance network is calculated, and then the DC OPF should be calculated to simulate the dispatching center operations addressing any overloaded lines. The DC OPF problem, formulated according to [9], aims to minimize both load shedding and changes in generation. Its constraints include overall power balance, line flow limits, generator limits, and load shedding limits. If the DC OPF solution is feasible, then the simulation of cascade n is terminated and cascade n+1 will be triggered by another initial outage, as long as the number of cascades has not yet reached $n_{\max}$; if not, then overloaded lines will be tripped by protection relays and the network needs to be updated to simulate potential line outages in the next iteration. The AC power flows in the i-th network can induce the i-th equilibrium of the system, i.e., $\mathbf{x}_s^{(i)}$. When updating the network in the (i+1)-th iteration, a new equilibrium $\mathbf{x}_s^{(i+1)}$ will be induced. However, the evaluation of the transient stability of the system, i.e., whether an existing equilibrium of the i-th network is in the DOA of a new equilibrium, i.e., $\mathbf{x}_s^{(i+1)}$ of the (i+1)-th network, cannot be evaluated using the original OPA model. To overcome this limitation, this paper proposes embedding an energy function into the existing framework of the OPA model to predict an out-of-step condition with generators, or in other words, transient instability.

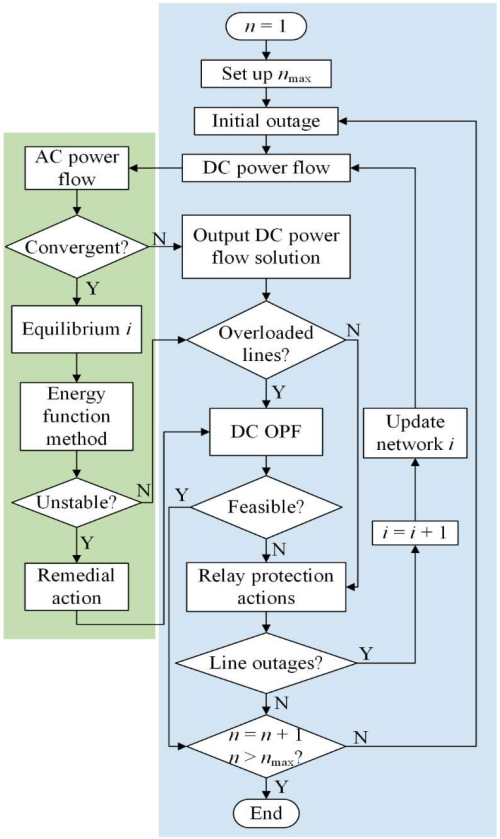

Fig. 1. The flowchart of the EF-QSS model.

As shown in the box on the left-hand side of Fig. 1, if the AC power flow calculation fails to lead to a feasible solution due to multiple line outages, the system should exit the energy function module and go back to the OPA model to find any overloaded lines based on the DC power flow. If the AC power flow solution is feasible, the energy function method is then employed to access the system's stability following a line outage. If the system is judged stable, it returns to the OPA model to find any overloaded lines based on the AC power flow. On the other hand, if the system is determined unstable, a control scheme is triggered to simulate the actual response to an out-of-step condition. In this paper, the assumed control scheme includes remedial action, generator redispatch, and load shedding. The remedial action trips the generator with the maximum rotor angle at the end of the short-term dynamic simulation. Then, generator redispatch and load shedding are performed by solving the DC OPF. The "Energy function method" box in Fig. 1 is illustrated in detail in Section II-C.

B. Power System Model

For the illustration purpose, the transient stability simulation adopting a sixth-order model in (1) [33] for all generators is considered to serve as a benchmark for the EF-QSS model.

$$\dot{\delta}_i = \omega_i - \omega_s,\ i = 1,2,\cdots,n \tag{1a}$$

$$2H_i\dot{\omega}_i = P_{mi} - P_{ei} - D_i(\omega_i - \omega_s) \tag{1b}$$

$$T'_{d0i}\dot{e}'_{qi} = E_{fdi} - (X_{di} - X'_{di})i_{di} - e'_{qi} \tag{1c}$$

$$T'_{q0i}\dot{e}'_{di} = (X_{qi} - X'_{qi})i_{qi} - e'_{di} \tag{1d}$$

$$T_{Ei}\dot{E}_{fdi} = K_{Ai}(V_{refi} - E_{ti}) - E_{fdi} \tag{1e}$$

$$T_{Gi}\dot{P}_{mi} = P_{refi} - P_{mi} - (\omega_i - \omega_s)/R_i \tag{1f}$$

The generator model (1) includes a fourth-order synchronous machine, a first-order exciter and a first-order governor [34].

In the energy function with the proposed EF-QSS model, the generator model (1) and load models are simplified by these assumptions [21]: 1) each generator is represented by a constant electromotive force E_i behind the d-axis transient reactance X'_{di} with saliency ignored; 2) each load is assumed to be a constant impedance load while each constant power or current load is approximated by the apparent impedance with the initial voltage at the bus; 3) the mechanical power of each generator is unchanged. By these assumptions, a simplified model of the n-generator system with the n-th generator as the reference is obtained, in which each generator adopts the classical model in (2), where G_{ij}+jB_{ij}=Y_{ij} is an element of the admittance matrix on the Kron-reduced network that only keeps generators' electromotive forces.

$$\dot{\delta}_{in} = \omega_{in},\ i = 1,2,\cdots,n-1 \tag{2a}$$

$$\dot{\omega}_{in} = \frac{1}{2H_i}\left(P_{mi} - P_{ei}\right) - \frac{1}{2H_n}\left(P_{mn} - P_{en}\right) - \lambda\omega_{in} \tag{2b}$$

$$\lambda = \frac{D_{ei}}{2H_i} \tag{2c}$$

$$\delta_{in} = \delta_i - \delta_n,\ \ i = 1,2,\cdots,n-1 \tag{2d}$$

$$\omega_{in} = \omega_i - \omega_n,\ \ i = 1,2,\cdots,n-1 \tag{2e}$$

$$P_{ei} = \mathrm{Re}\left[\tilde{E}_i^*\left(\sum_{j=1}^{n}(G_{ij} + \mathrm{j}B_{ij})\tilde{E}_j\right)\right],\ \ i = 1,2,\cdots,n \tag{2f}$$

$$E_i = \left|\tilde{E}_{ti0} + (R_{ai} + jX'_{di})\tilde{I}_{ti0}\right|,\ \tilde{E}_i = E_i\angle\delta_i \tag{2g}$$

Consider an artificial system (3) having only a half number of state variables of the reduced system modeled by (2). From [21], the types of equilibrium points of the artificial system are the same as those of the reduced system with small transfer conductances. Therefore, an equilibrium point of the reduced system can be obtained by finding the corresponding equilibrium point of the artificial system.

$$\dot{\delta}_{in} = P_{mi} - P_{ei} - \frac{H_i}{H_n}\left(P_{mn} - P_{en}\right) \ \stackrel{\text{def}}{=} f_i(\delta),\ \ i = 1,2,\cdots,n-1 \tag{3}$$

C. Energy Function Method under Line Outages

Consider the reduced system (2) subjected to a number of line outages. Following the i-th line outage, an energy function of the system is given by (4) according to [27], which consists of the kinetic energy V_{KE} and potential energy V_{PE} of the system.

$$V = V_{KE} + V_{PE} \tag{4a}$$

$$V_{KE} = \sum_{j=1}^{n-1}\sum_{k=j+1}^{n}\frac{H_jH_k}{H_T}\omega_{jk}^2 \tag{4b}$$

$$\begin{aligned} V_{PE} = &-\sum_{j=1}^{n-1}\sum_{k=j+1}^{n}\frac{1}{H_T}\left(P_j^{(i+1)}H_k - P_k^{(i+1)}H_j\right)(\delta_{jk} - \delta_{jk}^s) \\ &-\sum_{j=1}^{n-1}\sum_{k=j+1}^{n}C_{jk}^{(i+1)}(\cos\delta_{jk} - \cos\delta_{jk}^s) \\ &+\sum_{j=1}^{n-1}\sum_{k=j+1}^{n}D_{jk}^{(i+1)}\frac{\delta_{jn} + \delta_{kn} - (\delta_{jn}^s + \delta_{kn}^s)}{\delta_{jk} - \delta_{jk}^s}(\sin\delta_{jk} - \sin\delta_{jk}^s) \end{aligned} \tag{4c}$$

Here, superscript "(i+1)" indicates the (i+1)-th network topology after the i-th line outage; superscript "s" denotes the stable equilibrium point of the (i+1)-th network; $H_T = \sum_{j=1}^{n} H_j$; $P_j = P_{mj} - E_j^2 G_{jj}$; $C_{jk}^{(i+1)}$ and $D_{jk}^{(i+1)}$ are defined as:

$$C_{jk}^{(i+1)} = C_{kj}^{(i+1)} = E_k^{(i+1)}E_j^{(i+1)}B_{jk} \tag{5a}$$

$$D_{jk}^{(i+1)} = D_{kj}^{(i+1)} = E_k^{(i+1)}E_j^{(i+1)}G_{jk} \tag{5b}$$

The energy function determines the (i+1)-th network's DOA about its SEP, where the energy is zero with V_{KE}=V_{PE}=0, and an appropriately selected UEP on the boundary of the DOA determines the critical energy to be compared with the initial energy of the system after the line outage. If the initial energy is less, the system state can safely reach the SEP. In quasi-steady-state cascading outage simulations, the outage of each line is caused by its overload, not a short-circuit fault. The proposed EF-QSS model conducts a short-term time-domain simulation in order to find a relevant UEP for the line outage, which is similar to simulating the fault-on trajectory with the BCU method in [21] to find a CUEP.

The detailed flowchart of the "Energy function method" box in Fig. 1 is depicted in Fig. 2. When a line outage occurs, the initial state of the post-disturbance network is at the first local maximum point of the potential energy along the post-disturbance trajectory, i.e., $\mathbf{x}_1^*$. This state has zero kinetic energy and thus has the maximum potential energy. $\mathbf{x}_1^*$ is used as the initial guess to search for the relevant UEP by Newton's method. If it converges to the relevant UEP, the energy margin ΔV can be calculated, and the system's stability can be further evaluated based on ΔV. Otherwise, it converges to an SEP. If the SEP is different from the post-disturbance SEP, then the transient stability simulation is conducted for TSA; if the SEP is the same as the post-disturbance SEP, a time-domain simulation for a short time (e.g. 0.1 second) is conducted to obtain the post-disturbance trajectory. This is followed by the evaluation of the potential energy of the system along the trajectory. These two steps are repeated until the next local maximum point $\mathbf{x}_k^*$ of the potential energy along the post-disturbance trajectory is detected. Then, similarly, the new detected $\mathbf{x}_k^*$ will be utilized to search for the relevant UEP. Since $k_{\max}$ represents the maximum allowable number of searches, it indicates the maximum possible number of detected local maximum points. A larger $k_{\max}$ allows a more accurate estimation of the critical energy, but it also increases the simulation time. The search of the relevant UEP will terminate under three scenarios: 1) The relevant UEP is obtained; 2) The search converges to an SEP different from the post-disturbance SEP; 3) The number of searches reaches $k_{\max}$.

The latest local maximum point signifies the state of a system with the highest potential energy and the lowest kinetic energy

during the early stage of transient dynamics. It is found to be closest to the boundary of the DOA of the (i+1)-th network in the transient process following the i-th line outage. Therefore, this point is utilized as the initial guess to search for the relevant UEP by solving $f_i(\delta)$=0 using Newton's method.

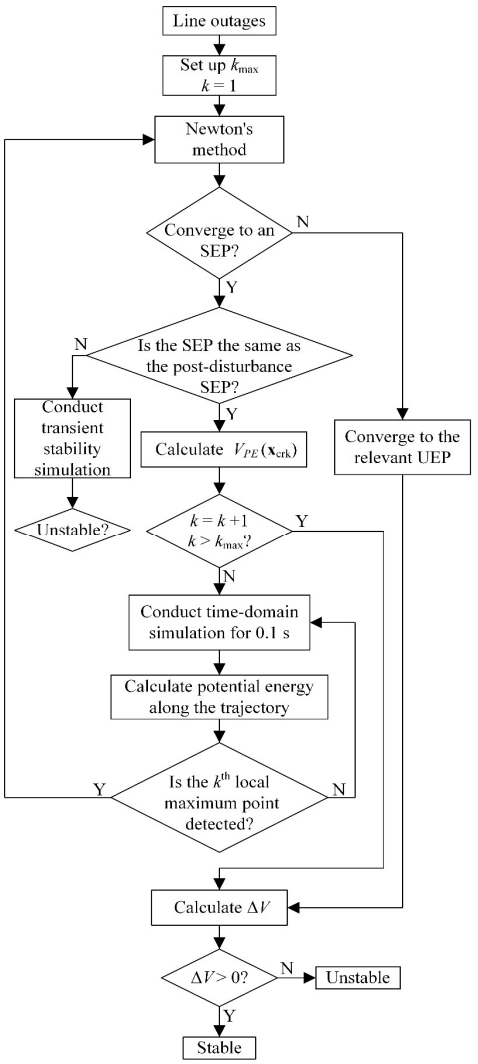

Fig. 2. The flowchart of the energy function method.

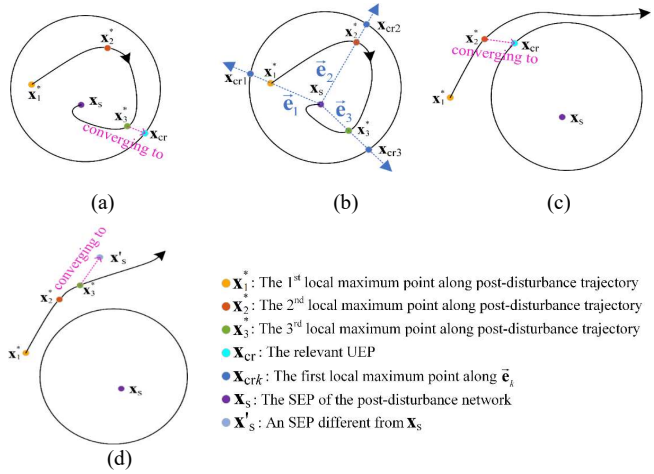

Fig.3. Four examples of search results: (a) converging to the relevant UEP for a stable case; (b) converging to $\mathbf{x}_S$ for a stable case; (c) converging to the relevant UEP for an unstable case; (d) converging to an SEP different from $\mathbf{x}_S$.

This approach is illustrated for four different, representative examples: **(a)**, **(b)**, **(c)** and **(d)** in **Fig. 3**. If the search converges to a UEP as shown in **Fig. 3 (a) or (c)**, the critical energy V_{cr} can be calculated by substituting the UEP value into (4c). Since the initial point of the (i+1)-th network, $\mathbf{x}_1^*$, is within the DOA of the (i+1)-th network in Fig. 3 (a), it represents a stable case. In contrast, $\mathbf{x}_1^*$ is outside the DOA of the (i+1)-th network in Fig. 3 (c), representing an unstable case. If the search converges to the SEP of the (i+1)-th network, as depicted in **Fig. 3 (b)**, the critical energy V_{cr} is estimated by identifying the minimum value among the potential energies at the first local maximum point $\mathbf{x}_{crk}$ along all paths defined by the unit vector $\vec{\mathbf{e}}_k$ for different k at a step of h in (6), starting from the SEP of the (i+1)-th network, i.e., $\mathbf{p}_0$=$\mathbf{x}_S$. For example, as illustrated in **Fig. 3 (b)**, V_{cr} = min $\{V_{PE}(\mathbf{x}_{cr1}), V_{PE}(\mathbf{x}_{cr2}), V_{PE}(\mathbf{x}_{cr3})\}$.

$$\vec{\mathbf{e}}_k = \frac{\mathbf{x}_s - \mathbf{x}_k^*}{\left\|\mathbf{x}_s - \mathbf{x}_k^*\right\|} \tag{6a}$$

$$\mathbf{p}_{M+1} = \mathbf{p}_M + h\vec{\mathbf{e}}_k \tag{6b}$$

where $\|\cdot\|$ represents the norm operator of a vector; h is set to 0.2 in this paper. If the search converges to an SEP different from the SEP of the (i+1)-th network, denoted as $\mathbf{x}'_S$, as depicted in **Fig. 3 (d)**, conduct transient stability simulation for TSA. The energy margin of the post-disturbance system is

$$\Delta V = V_{cr} - V_{PE}(\mathbf{x}_1^*) \tag{7}$$

where $\mathbf{x}_1^*$ represents the first local maximum point of the potential energy along the post-disturbance trajectory, and it is also the SEP of the i-th network. If ΔV is greater than zero, the system is considered stable; otherwise, it is unstable.

III. Numerical Experiments on the EF-QSS Model

To validate the proposed EF-QSS model in predicting transient instability during a cascading process, this section presents its numerical experiments conducted on the NPCC 140-bus system shown in Fig. 4, which is a test bed developed by [35] for cascading outage simulations.

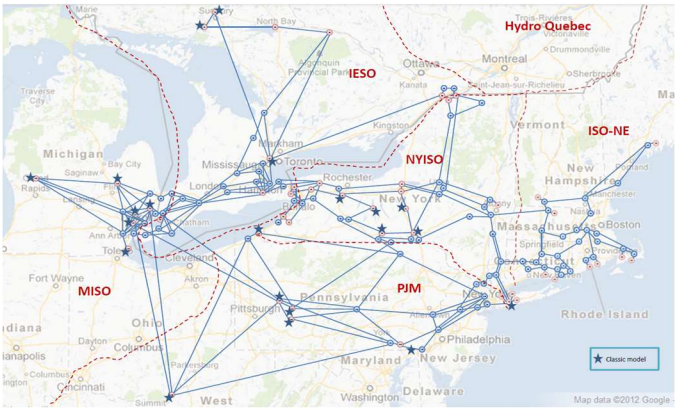

Fig. 4. NPCC 140-bus system.

To assess the accuracy and efficiency of cascading outage simulations using the proposed EF-QSS model, another model referred to as "TS-OPA" is used, which follows the same flowchart as Fig. 1 except for replacing the energy function method with a time-domain transient stability simulation adopting the detailed model given in (1) for TSA. All

subsequent accuracy assessments of the EF-QSS model are compared with those of the TS-OPA model. The transient stability simulation is terminated (typically in 10-20 seconds following a switch) once satisfying either condition in (8):

$$\Delta\delta_{\max} > \delta_u \tag{8a}$$

$$\left\|\dot{x}\right\|_\infty \le \epsilon \tag{8b}$$

where (8a) judges the case to be unstable when $\Delta\delta_{\max}$ exceeds δ_u; (8b) judges the case to be stable if the derivatives of all state variables are within a tolerance ϵ. The case is judged stable if the simulation reaches $T_{\max}$. In this paper, δ_u, ϵ, and $T_{\max}$ are set to 2π, 10^{-3}, and 20 s, respectively.

The energy function is derived for the reduced system modeled by (2), while benchmarked with the detailed model in (1). To examine the influence of the model differences on TSA, 10,000 "N-2" cascade events on the NPCC system under the base load condition are simulated. Here, "N-2" refers to initial outages that trip two lines. Their TSAs shown in Table I are obtained using transient stability simulations adopting the detailed model and the reduced model, respectively. As observed from Table I, the influence of model difference on TSA is insignificant, and thus the energy function from the reduced system can be employed here for the TSA requirements with the proposed EF-QSS model.

In the rest of this section, Section III-A illustrates how to conduct cascade simulation using the proposed EF-QSS model. Section III-B analyzes the influence of the model's parameter on its accuracy and time performance. Section III-C examines the model's performance under different loading conditions. Furthermore, Section III-D evaluates the performance of the model under different numbers of initial line outages. Finally, Section III-E compares the severities of the cascading outages generated by the proposed EF-QSS model, the original OPA model, and the TS-OPA model based on two metrics: the average number of line outages and the average amount of load shedding.

TABLE I
TSA FROM SIMULATIONS USING DIFFERENT MODELS

TSA		Reduced model	
		Stable (68.55%)	Unstable (31.45%)
Detailed model	Stable (68.78%)	68.41%	0.37%
	Unstable (31.22%)	0.14%	31.08%

A. Illustration of the EF-QSS Model

To illustrate how TSA is performed by the proposed EF-QSS model using the energy function method that finds up to $k_{\max}$=3 local maximum points, three examples are shown in Fig. 5, Fig. 6, and Fig. 7, respectively. The TSA result of each stage is compared with the ground truth from a time-domain simulation.

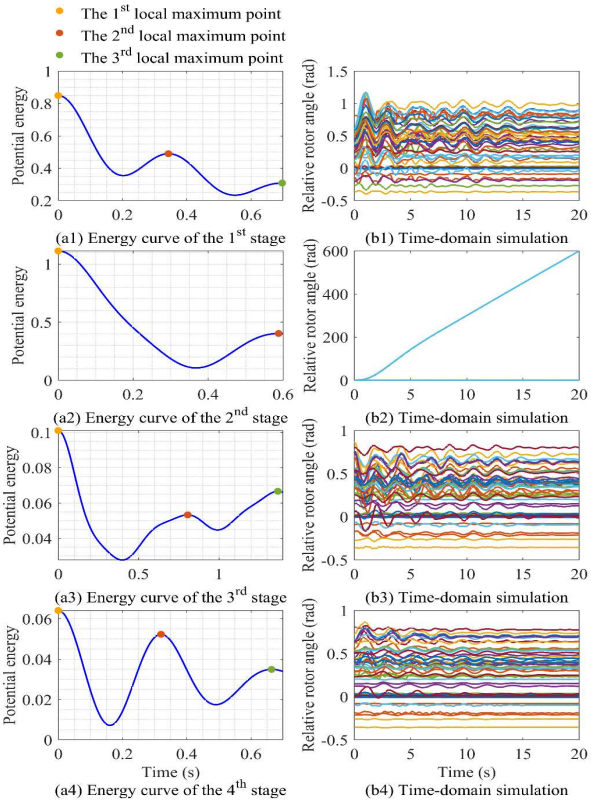

Fig. 5. Analysis of a cascade event with four stages.

The first example records a cascading process with four stages: 1) the initial outages of lines 65 and 74, 2) the outage of line 78, 3) the concurrent outages of lines 79 and 80, 4) the outage of line 81. Thereafter, the cascade stops because of no further overloading. Throughout this process, the network topology is changed four times, resulting in four different potential energy curves as shown by (a1)-(a4) in Fig. 5, which are obtained by calculating potential energy along the short-term post-disturbance trajectory. The search results of (a1), (a3) and (a4) in Fig. 5 all correspond to the scenario shown in Fig. 3 (b), resulting in a positive energy margin, whereas the search result of Fig. 5 (a2) corresponds to the scenario shown in Fig. 3 (c), resulting in a negative energy margin. Therefore, the energy function module in the EF-QSS model predicts the system to be stable, unstable, stable, and stable respectively for the four stages. The ground truth of TSA for each stage is obtained by time-domain simulation, shown in Fig. 5 (b1)-(b4), respectively, indicating the system is stable, unstable, stable, and stable respectively for the four stages, which verifies that the EF-QSS model makes accurate TSAs for this cascade event.

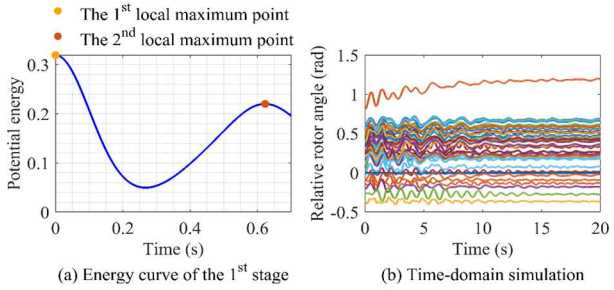

Fig. 6. Analysis of a cascade event with one stage.

Similarly, Fig. 6 shows a second cascade event with initial outages of lines 18 and 44, lasting for only one stage due to no further overloading. Fig. 6 (a) shows potential energy along the short-term post-disturbance trajectory, corresponding to the scenario shown in Fig. 3 (a). The search converges to the relevant UEP, resulting in a positive energy margin. Thus, the EF-QSS model predicts the system to be stable, which matches the TSA determined by time-domain simulation shown in Fig. 6 (b).

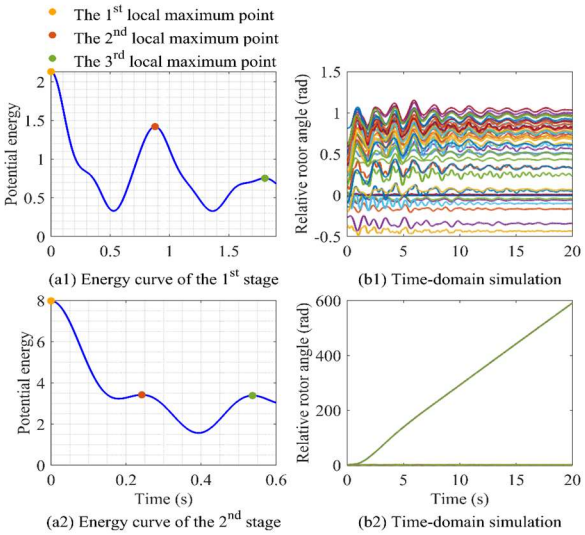

Fig. 7. Analysis of a cascade event with two stages.

Fig. 7 shows a third cascade event with two stages: 1) the initial outages of lines 33 and 92, 2) the concurrent outages of lines 27, 28, 30,78, and 100. The cascade then stops due to no further overloading following the remedial action. The search result of Fig. 7 (a1) corresponds to the scenario shown in Fig. 3 (b), resulting in a positive energy margin, while the search result of Fig. 7 (a2) corresponds to the scenario shown in Fig. 3 (d), necessitating transient stability simulation for TSA. Therefore, the EF-QSS model predicts the system to be stable and unstable for the two stages, respectively, matching the TSA results from simulations shown in Fig. 7 (b1)-(b2). The accuracy of the EF-QSS model will be further evaluated across a large number of cascades in the following sections.

B. Parameter Influence

1) Influence on Accuracy

TABLE II
PERFORMANCE WITH DIFFERENT k_{max}

k_{max}	Accuracy	
	Stable cases classified as stable	Unstable cases classified as unstable
2	99.72%	95.78%
3	99.52%	99.66%

To evaluate how parameter k_{max} influences the TSA accuracy of the proposed energy function method in the EF-QSS model, 10,000 "N-2" cascade events on the NPCC system under the base load condition are simulated for each k_{max} value. The benchmark results are obtained from the TS-OPA model. Table II shows the performance of the energy function method with different k_{max} values. k_{max}=3 results in higher TSA accuracy than k_{max} =2 especially for unstable cases. This is because k_{max}=3 takes both the first and second swings into considerations, resulting in more accurate critical energy while k_{max} = 2 only considers the first swing.

2) Influence on Time Performance

To evaluate the time performance of the EF-QSS model, two comparisons were conducted with the TS-OPA model. The first comparison focused on the duration of time-domain simulations, specifically the length of the time window required for TSA during cascading outage simulations. The second comparison evaluates the time cost, which refers to the computing time.

10,000 "N-2" cascade events are simulated using the TS-OPA and EF-QSS models with k_{max}=2 and 3, respectively. The average duration of time-domain simulations using the TS-OPA is 14.11 seconds. Using the EF-QSS model, only 5.31% of the cases with k_{max}=2 and 6.85% of the cases with k_{max}=3 need to conduct transient stability simulations. Excluding these cases, Fig. 8 shows the distribution of the durations of time-domain simulations that are required by the energy function method using the EF-QSS model. From Fig. 8 (a), for k_{max}=2, around 80% of the cases can employ the energy function method for TSA with a time-domain simulation of only 0.6 s or less. From Fig. 8 (b), for k_{max}=3, around 70% of the cases can employ the energy function method for TSA using a time-domain simulation of 0.7 s or less. The average simulation duration is 0.51 s for k_{max}=2 and 0.81 s for k_{max}=3. Both are significantly less compared with the average duration of simulations with the TS-OPA model, demonstrating the high efficiency of the EF-QSS model for TSA with cascading outages compared to the TS-OPA model. This merit with the EF-QSS model can potentially save significant time in the real-time operating environment when online simulations of cascading outages are required for preventive and mitigative control strategies.

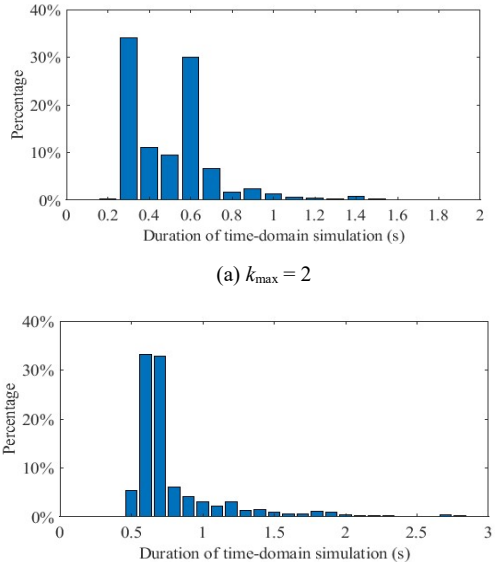

Fig. 8. Distribution of simulation durations for the EF-QSS model with energy function method.

In MATLAB on a desktop computer with Intel core i7 CPU and 16GB RAM, the total time costs for generating the 10,000 "N-2" cascade events using the TS-OPA model and the EF-QSS model are estimated and compared in Table III. The EF-QSS model achieves a significant reduction of the time cost by 78.4% and 69.7% for k_{max}=2 and 3, respectively. This further validates the high efficiency of the EF-QSS model in generating large datasets of cascading outages.

TABLE III
COMPARISON OF TIME COSTS BETWEEN DIFFERENT MODELS

Model	TS-OPA	EF-QSS	
		k_{max} = 2	k_{max} = 3
Time cost	12.68 hours	2.74 hours	3.84 hours

To further demonstrate the significant speedup by using the EF-QSS model for simulations of cascading outages, full time-domain simulations are also conducted as benchmarks. In each full time-domain simulation, a dynamic model of the power system using the detailed generator model in (1) is continuously solved, and the same remedial action, DC OPF-based mitigation control, and relay protection scheme as shown in Fig. 1 are conducted upon any overloading or detected transient instability. Unlike the TS-OPA model, which terminates its time-domain simulation once transient stability is determined, each new full time-domain simulation of cascading outages aims to replicate the real evolution of a cascade by continuing the simulation from its initial fault or switch until the cascade concludes. According to analyses of the 2003 Northeast blackout [19], [36]-[38], cascade events caused by line overloading typically take around 30 minutes to evolve from the beginning of one stage to the next in a lightly stressed system but can progress within just a few minutes in a highly stressed system. To represent these varying evolution speeds, two new cases of cascades are studied by full time-domain simulations. Case 1, representing a slow evolution, operates under the base loading condition, whose cascade is initiated by outages of lines 31 and 124, progressing through four stages. The evolution time between stage 1 and stage 2 is set at 30 minutes, decreasing progressively to 25, 20, and 15 minutes in subsequent stages as the system becomes increasingly stressed. Case 2, representing a fast evolution, operates under a heavier loading condition, with a 50% increase over the base load of each bus. The cascade is initiated by outages of lines 8 and 36, progressing through three stages. The evolution time between stage 1 and stage 2 is set at 7 minutes, dropping sharply to 2 minutes and 1 minute in the following stages.

TABLE IV
COMPARISON OF TIME COSTS FOR TWO CASES

Model		Time cost (s)	
		Case 1	Case 2
Dynamic model		257.1	31.1
TS-OPA		8.9	8.3
EF-QSS	k_{max} = 2	2.8	2.6
	k_{max} = 3	3.2	3.8

Table IV presents the time costs for these two new cases simulated using three different models. The EF-QSS model achieves the smallest time costs in both cases. In contrast, the dynamic model is highly time-consuming, requiring over 80 times the computation time of the EF-QSS model for Case 1 and 8 times for Case 2. Although the TS-OPA model reduces time costs significantly compared to the dynamic model, it remains inefficient for simulating a large number of cascades, as demonstrated in Table III. Compared to the case with k_{max}=2, the EF-QSS model with k_{max}=3 has better accuracy with only a slight increase in time cost. Therefore, in the rest of the paper, k_{max} is set to 3 to achieve higher accuracy.

C. Considering Different Loading Conditions

The performance of the EF-QSS model is evaluated under three loading conditions with load factors of 1.0, 1.2 and 1.5, as shown in Table V, which respectively consider the base case and the system loads increased evenly to 1.2 and 1.5 times. To account for load variations and uncertainties, each bus load under a certain loading condition is further varied by a factor following a uniform distribution between the range of [0.9, 1.1]. For each loading condition, the EF-QSS model is used to simulate 10,000 "N-2" cascade events on the NPCC system. The benchmark results are obtained from the TS-OPA model. As shown in Table V, the accuracy of TSA basically remains consistent across different loading conditions with only slight variations, which demonstrates the robustness of the EF-QSS model under variations in loads.

TABLE V
PERFORMANCE UNDER DIFFERENT LOADING CONDITIONS

Load factor	Accuracy	
	Stable cases classified as stable	Unstable cases classified as unstable
1.0	99.52%	99.66%
1.2	99.36%	99.63%
1.5	99.34%	99.57%

D. Considering Various Initial Failures

In this section, the performance of the EF-QSS model is evaluated considering different numbers of initial line outages. The results are presented in Table VI, which compares the accuracy of the model with initial "N-2" and "N-3" line outages.

TABLE VI
PERFORMANCE WITH DIFFERENT NUMBERS OF INITIAL LINE OUTAGES

Initial failures	Accuracy	
	Stable cases classified as stable	Unstable cases classified as unstable
"N-2"	99.52%	99.66%
"N-3"	99.32%	99.08%

Table VI shows the TSA accuracies for both stable and unstable cases for each type of scenario. It is observed that the accuracy of the model exhibits slight and acceptable differences between the "N-2" and "N-3" scenarios, for both stable and unstable cases. This indicates that the EF-QSS model maintains good accuracy for scenarios with different numbers of initial line outages, highlighting the robustness of the EF-QSS model.

E. Statistical Comparisons

This section provides statistical comparisons between different models, focusing on comparing two key indices on the severity of cascading outages: the average number of line outages and the average amount of load shedding. The OPA, TS-OPA, and EF-QSS models are used to each simulate 10,000 "N-2" cascade events under the base load condition, with the TS-OPA model serving as the benchmark. The statistical comparisons between these models are presented in Table VII. The result indicates that the EF-QSS model approximately matches with the TS-OPA model in terms of both severity indices, thereby further validating the accuracy of the EF-QSS model. However, the OPA model exhibits significantly lower values for both indices than the EF-QSS and TS-OPA models. This discrepancy can be attributed to the OPA model's limitation in neglecting transient dynamics and optimistically assuming that all line outages do not lead to transient instability issues. Thus, the OPA model underestimates the propagation and consequences of cascading outages. In contrast, the EF-QSS model addresses this limitation by incorporating the energy function module into the OPA model to enable efficient TSA without conducting transient stability simulations. By addressing transient stability in cascading outage simulations, the EF-QSS model can generate more accurate cascading outage cases statistically close to those generated from the TS-OPA model. These findings highlight the significance of accounting for transient dynamics in the simulation of cascading outages to generate more realistic and accurate cascading outage data.

TABLE VII
STATISTICAL COMPARISONS BETWEEN DIFFERENT MODELS

Model	Average number of line outages	Average amount of load shedding (MW)
OPA	6.64	356.44
TS-OPA	12.42	2355.69
EF-QSS	13.87	2684.42

IV. CONCLUSIONS

This paper proposed an EF-QSS model as a novel approach for simulation of cascading outages in power grids. By integrating the energy function method into the framework of a quasi-steady-state cascading model, the proposed new model offers an efficient and effective solution for addressing transient stability concerns in simulations of cascading outages. The accuracy of the proposed EF-QSS model is validated on the NPCC 140-bus system. The performance evaluations of the EF-QSS model under different loading conditions and varying numbers of initial line outages show consistent accuracy, with only a slight variation, indicating the effectiveness and robustness of the model in capturing transient dynamics during cascading outages. Statistical comparisons between the OPA, TS-OPA, and EF-QSS models reveal that the OPA model underestimates the severity of cascade outages due to its neglect of transient dynamics. This emphasizes the significance of considering transient effects in simulating cascading outages to generate more realistic and accurate cascading outage data. Furthermore, the efficiency of the EF-QSS model is examined. The results show that the proposed EF-QSS model achieves a significant reduction in time costs compared to the TS-OPA and dynamic models, highlighting the high efficiency of the EF-QSS model in conducting TSA for cascading outages. Thus, the EF-QSS model has the potential to save significant time for real-time applications to help prevent or mitigate the propagation of cascading outages.

V. REFERENCES

[1] I. Dobson, B. A. Carreras, D. E. Newman, "A loading-dependent model of probabilistic cascading failure," *Probability in the Engineering and Informational Sciences*, vol. 19, no. 1, pp. 15-32, Jan. 2005.

[2] J. Kim, I. Dobson, "Approximating a loading-dependent cascading failure model with a branching process," *IEEE Trans. Reliability*, vol. 59, no. 4, pp. 691-699, Dec. 2010.

[3] I. Dobson, "Estimating the propagation and extent of cascading line outages from utility data with a branching process," *IEEE Trans. Power Syst.*, vol. 27, no. 4, pp. 2146-2155, Apr. 2012.

[4] J. Qi, K. Sun, S. Mei, "An interaction model for simulation and mitigation of cascading failures," *IEEE Trans. Power Syst.*, vol. 30, no. 2, pp. 804-819, Mar. 2015.

[5] J. Qi, J. Wang, K. Sun, "Efficient estimation of component interactions for cascading failure analysis by EM algorithm," *IEEE Trans. Power Syst.*, vol. 33, no. 3, pp. 3153-3161, May 2018.

[6] W. Ju, K. Sun, J. Qi, "Multi-layer interaction graph for analysis and mitigation of cascading outages," *IEEE J. Emerg. Sel. Topics in Circuits Syst.*, vol. 7, no. 2, pp. 239-249, Jun. 2017.

[7] P. D. H. Hines, I. Dobson, P. Rezaei, "Cascading power outages propagate locally in an influence graph that is not the actual grid topology," *IEEE Trans. Power Syst.*, vol. 32, no. 2, pp. 958-967, Mar. 2017.

[8] K. Zhou, I. Dobson, Z. Wang, et al, "A Markovian influence graph formed from utility line outage data to mitigate large cascades," *IEEE Trans. Power Syst.*, vol. 35, no. 4, pp. 3224-3235, Jul. 2020.

[9] I. Dobson, B. A. Carreras, V. E. Lynch, D. E. Newman, "An initial model for complex dynamics in electric power system blackouts," in *Proc. 34th Hawaii Int. Conf. Syst. Sci.*, Maui, HI, USA, Jan. 2001, pp. 710-718.

[10] S. Mei, F. He, X. Zhang, S. Wu, G. Wang, "An improved OPA model and blackout risk assessment," *IEEE Trans. Power Syst.*, vol. 24, no. 2, pp. 814-823, May 2009.

[11] B. A. Carreras, D. E. Newman, I. Dobson, N. S. Degala, "Validating OPA with WECC data," in *Proc. 46th Hawaii Int. Conf. Syst. Sci.*, Wailea, HI, USA, Jan. 2013, pp. 2197-2204.

[12] W. Ju, K. Sun, R. Yao, "Simulation of cascading outages using a power-flow model considering frequency," *IEEE Access*, vol. 6, pp. 37784-37795, Jun. 2018.

[13] B. Park, X. Su, K. Sun, "An enhanced OPA model: incorporating dynamically induced cascading failures," *IEEE Trans. Power Syst.*, vol. 37, no. 6, pp. 4962-4965, Nov. 2022.

[14] M. A. Rios, D. S. Kirschen, D. Jayaweera, et al, "Value of security: modeling time-dependent phenomena and weather conditions," *IEEE Trans. Power Syst.*, vol. 17, no. 3, pp. 543-548, Aug. 2002.

[15] A. G. Phadeke, J. S. Thorp, "Expose hidden failures to prevent cascading outages," *IEEE Comput. Appl. Power*, vol. 9, no. 3, pp. 20-23, Jul. 1996.

[16] J. Song, E. Cotilla-Sanchez, G. Ghanavati, P. D. Hines, "Dynamic modeling of cascading failure in power systems," *IEEE Trans. Power Syst.*, vol. 31, no. 3, pp. 2085-2095, Jun. 2015.

[17] P. Henneaux, P. E. Labeau, J. C. Maun, "A level-1 probabilistic risk assessment to blackout hazard in transmission power systems," *Reliability Engineering & System Safety*, pp. 41-52, Jun. 2012.

[18] P. Henneaux, P. E. Labeau, J. C. Maun, L. Haarla, "A two-level probabilistic risk assessment of cascading outages," *IEEE Trans. Power Syst.*, vol. 31, no. 3, pp. 2393-2403, May 2016.

[19] R. Yao, S. Huang, K. Sun, F. Liu, X. Zhang, S. Mei, "A multi-timescale quasi-dynamic model for simulation of cascading outages," *IEEE Trans. Power Syst.*, vol. 31, no. 4, pp. 3189-3201, Jul. 2016.

[20] T. Odun-Ayo, M. L. Crow, "Structure-preserved power system transient stability using stochastic energy functions," *IEEE Trans. Power Syst.*, vol. 27, no. 3, pp. 1450-1458, Aug. 2012.

[21] H. D. Chiang, F. F. Wu, P. P. Varaiya, "A BCU method for direct analysis of power system transient stability," *IEEE Trans. Power Syst.*, vol. 9, no. 3, pp. 1194-1208, Aug. 1994.

[22] Y. Xue, T. Van Custem, M. Ribbens-Pavella, "Extended equal area criterion justifications, generalizations, applications," *IEEE Trans. Power Syst.*, vol. 4, no. 1, pp. 44-52, Feb. 1989.

[23] T. L. Vu, K. Turitsyn, "Lyapunov functions family approach to transient stability assessment," *IEEE Trans. Power Syst.*, vol. 31, no. 2, pp. 1269-1277, Mar. 2016.

[24] T. L. Vu, et al, "Toward simulation-free estimation of critical clearing time," *IEEE Trans. Power Syst.*, vol. 31, no. 6, pp. 4722-4731, Nov. 2016.

[25] S. M. Al Araifi, M. S. E. Moursi, S. M. Djouadi, "Individual functions method for power system transient stability assessment," *IEEE Trans. Power Syst.*, vol. 35, no. 2, pp. 1264-1273, Mar. 2020.

[26] C. Mishra, A. Pal, J. S. Thorp, V. A. Centeno, "Transient stability assessment of prone-to-trip renewable generation rich power systems using Lyapunov's direct method," *IEEE Trans. Sustain. Energy*, vol. 10, no. 3, pp. 1523-1533, Jul. 2019.

[27] T. Athay, R. Podmore and S. Virmani, "A practical method for direct analysis of transient stability," *IEEE Trans. Power App. Syst.*, vol. PAS-98, no. 2, pp. 573-584, Mar. 1979.

[28] H. D. Chiang, *Direct Methods for Stability Analysis of Electric Power Systems: Theoretical Foundation, BCU Methodologies, and Applications*. New York, NY, USA: Wiley, Mar. 2011.

[29] A. A. Fouad, V. Vittal, O. Taekyoo, "Critical energy for transient stability assessment of a multimachine power system," *IEEE Trans. Power App. Syst.*, vol. PAS-103, no. 8, pp. 2199-2206, Aug. 1984.

[30] A. A. Fouad, S. E. Stanton, K. R. C. Mamandur, "Contingency analysis using the transient energy margin technique," *IEEE Trans. Power App. Syst.*, vol. PAS-101, no. 4, pp. 757-766, Apr. 1982.

[31] M. L. Scala, R. Sbrizzai, F. Torelli, P. Scarpellini, "A tracking time domain simulator for real-time transient stability analysis," *IEEE Trans. Power Syst.*, vol. 13, no. 3, pp. 992-998, Aug. 1998.

[32] R. Zarate-Minano, T. Van Cutsem, F. Milano, A. J. Conejo, "Securing transient stability using time-domain simulations within an optimal power flow," *IEEE Trans. Power Syst.*, vol. 25, no. 1, pp. 243-253, Feb. 2010.

[33] B. Wang, K. Sun, "Formulation and characterization of power system electromechanical oscillations," *IEEE Trans. Power Syst.*, vol. 31, no. 6, pp. 5082-5093, Nov. 2016.

[34] Y. Liu, K. Sun, R. Yao, B. Wang, "Power system simulation using a differential transformation method," *IEEE Trans. Power Syst.*, vol. 34, no. 5, pp. 3739-3748, 2019.

[35] W. Ju, J. Qi, K. Sun, "Simulation and analysis of cascading failures on an NPCC power system test bed," in *Proc. IEEE Power Energy Soc. General Meeting*, Denver, CO, USA, Jul. 2015, pp. 1-5.

[36] A. Muir, J. Lopatto, *Final Report on the August 14, 2003 Blackout in the United States and Canada: Causes and Recommendations*, U.S.-Canada Power System Outage Task Force, Washington, DC, USA, Apr. 2004.

[37] K. Sun, *Cascading Failures in Power Grids: Risk Assessment, Modeling, and Simulation*. Springer, 2024.

[38] Z. Guo, K. Sun, X. Su, S. Simunovic, "A review on simulation models of cascading failures in power systems," *iEnergy*, vol. 2, no. 4, pp. 284-296, Dec. 2023.

Zhenping Guo (Student Member, IEEE) received her B.S. and M.S. degrees in electrical engineering from Wuhan University of Technology, Wuhan, China, in 2013, and Wuhan University, Wuhan, China, in 2016, respectively. She is currently pursuing a Ph.D. degree with the Department of Electrical Engineering and Computer Science, University of Tennessee, Knoxville, TN, USA. From 2016 to 2021, she was an Engineer with the State Grid Hubei Power Supply Company. Her research interests include cascading failures, power system simulations, and transient stability analysis.

Xiaowen Su joined the ISO-NE Transmission Service, Model Administration, and Support team in 2024. She earned her Ph.D. in Mechanical Engineering from the University of Tennessee, Knoxville, in 2019, specializing in rotor dynamics and control. From 2019 to 2024, she held research positions at Texas A&M University and the University of Tennessee, Knoxville, culminating in her role as Assistant Professor of Research in the Electrical and Computer Engineering Department at the University of Texas at San Antonio. Her research interests include power system cascading failure analysis, GMD studies, and SC studies.

Kaiyang Huang (Graduate Student Member, IEEE) received the B.S. degree in electrical engineering from North China Electric Power University, China, in 2020. He is currently pursuing the Ph.D. degree at the Department of Electrical Engineering and Computer Science, University of Tennessee, Knoxville, USA. His research interests include power system simulation, transient stability analysis, and dynamics.

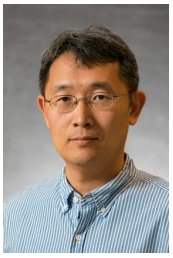

Kai Sun (Fellow, IEEE) is a professor in the Department of Electrical Engineering and Computer Science at the University of Tennessee, Knoxville, USA. He received his B.S. degree in Automation in 1999 and his Ph.D. degree in Control Science and Engineering in 2004, both from Tsinghua University, Beijing, China. From 2007 to 2012, he served as a Project Manager in grid operations, planning, and renewable integration at the Electric Power Research Institute (EPRI), Palo Alto, CA.

Srdjan Simunovic is a Distinguished Research Staff with the Computational Sciences and Engineering Division, Oak Ridge National Laboratory, Oak Ridge, TN, USA. He has M.Sc. and Ph.D. degrees in civil engineering from Carnegie Mellon University, Pittsburgh, PA, USA. His research expertise includes applied mathematics for multi-scale and multi-physics problems, parallel algorithms and computing, energy storage, and computational modeling of materials and processes.

Hsiao-Dong Chiang (Life Fellow, IEEE) received the Ph.D. degree in electrical engineering and computer sciences from the University of California at Berkeley, Berkeley, CA, USA. Since 1998, he has been a Professor with the School of Electrical and Computer Engineering, Cornell University, Ithaca, NY, USA. He is the Founder of Bigwood Systems Inc., Ithaca, NY, USA. His current research interests include nonlinear system theory, nonlinear computation, nonlinear optimization, and their practical applications. He was an associate editor of several IEEE TRANSACTIONS and IEEE journals and a Board Member of the Institute of Electrical Engineers of Japan (IEEJ).